



## AN EXPERIMENTAL STUDY ON THE EFFICIENCY OF CHROMIUM (VI) REMOVAL WITH STARCH-MAGNETITE NANOCOMPOSITE (Starch@MNPs)

Rojin ŞİMŞEK<sup>1</sup>, Busra Nur ÇİFTÇİ<sup>1</sup>, Yağmur UYSAL<sup>1\*</sup>

<sup>1</sup> Department of Environmental Engineering, Engineering Faculty, Mersin University, Mersin, Turkey.

### ABSTRACT

Nowadays, magnetic nanoadsorbents are used commonly in the removal of heavy metal ions from wastewater. In this study, we prepared starch-coated magnetic nanoparticles (Starch@MNPs) by the co-precipitation method, and used to remove Cr(VI) ions from water. Several batch experiments were performed to determine optimum conditions in the adsorption studies for Starch@MNPs such as pH, contact time, temperature, chromium ion and adsorbent concentrations. The synthesized Starch@MNPs were analyzed by Scanning Electron Microscopy (SEM) to illustrate the shape and surface properties of the nanoparticles. In order to define characterization of the adsorbent, Fourier-transform Infrared Spectroscopy (FTIR) and Energy Dispersive X-Ray Analysis (EDX) techniques were also used. The experimental data were compared with isotherm and kinetic models in order to determine the most suitable for fitting. The results showed that Cr (VI) adsorption of Starch@MNPs was more suitable for Temkin isotherm and Pseudo-second kinetic model, respectively. The maximum adsorption efficiency (98%) of Cr (VI) in 10 mg/L initial concentration was obtained at contact time of 60 min., pH 4.0 and adsorbent concentration of 2.0 g/L. The obtained data from the study showed that Starch@MNPs have quite high separation efficiency for Cr(VI) ions and also showed that this adsorbent can be used as a promising adsorbent in future adsorption studies.

**Keywords:** Adsorption, Chromium, Nanocomposite, Magnetite, Starch

### 1. INTRODUCTION

The recent advances in nanotechnology have enabled nanomaterials to be used in many areas. Nanomaterials are generally unstable and have a tendency to agglomerate. During the production stage of nanomaterials, researchers can control the chemical composition, size and shape of them by improving the already superior properties of nanomaterials or gaining new physical and chemical properties. Magnetite ( $Fe_3O_4$ ) is one of the leading nanomaterials in which many studies have been carried out in terms of its strong magnetic properties which enable it to be separated easily from water and non-toxic structure. Due to these properties, there are many researches focusing on magnetite nanoparticles for applications in water and wastewater treatment or for the removal of specific pollutants from water [1]. Although many different methods are used in the synthesis of magnetite, co-precipitation technique is one of the simple, inexpensive and effective methods. In this method, magnetite nanoparticles are produced by combining the iron ions charged with +2 and +3 in basic solution under high temperature and nitrogen medium.

In recent years, there has been an increasing trend in the synthesis of materials with green chemistry and the use of these materials in many industrial applications, including wastewater treatment. Green synthesis applications can eliminate or reduce the harm of many dangerous substances. In these applications, biopolymers are preferred both by themselves and with the materials they are brought together in terms of easy degradability, renewability and compatibility with living things. The most preferred polymers among these are cellulose, starch, chitosan and plant extracts. Recently, the use of natural starches has become significant in green synthesis methods of nanomaterials and nanocomposites [2, 3]. Starch is one of the most abundant naturally occurring polysaccharides with low

\*Corresponding Author: [yuysal@mersin.edu.tr](mailto:yuysal@mersin.edu.tr)

Received: 22.11.2019 Published: 15.06.2020

cost and nontoxicity, and it can also be abundant in the wastewater of many industries, such as the chips and paper industries.

Adsorption is a method that has high removal efficiency and easy to use. This method has been used for the removal of many pollutants from wastewaters to date and often successful results have been obtained. Another advantage of this process is the ability to regenerate the adsorbent material by the appropriate desorption process and to be able to be used several times without losing the high removal efficiency. In this present work, starch/magnetite ( $\text{Fe}_3\text{O}_4$ ) composites (Starch@MNPs) were synthesized as adsorbent materials to adsorb and separate Cr(VI) ions from an aqueous solution. The important factors affecting the adsorption efficiency such as solution pH, contact time, and initial Cr(VI) concentrations were investigated. The Langmuir, Freundlich and Temkin isotherm models were also used to determine the equilibrium of the adsorption process. Kinetic adsorption experiments were carried out to establish the effect of time on the adsorption process and to determine the adsorption rate for Cr(VI) removal.

## 2. MATERIAL AND METHODS

### 2.1. Reagents and Chemicals

Cr(VI) stock solution (1000 mg/L) was prepared using  $\text{K}_2\text{Cr}_2\text{O}_7$  (Riedel-de Haen).  $\text{NH}_4\text{OH}$ ,  $\text{FeCl}_3 \cdot 6\text{H}_2\text{O}$  and  $\text{FeSO}_4 \cdot 7\text{H}_2\text{O}$  (Merck), which are required in the synthesis of magnetite nanocomposite was analytically grade. 0.1M HCl and NaOH were used for pH adjustments.

### 2.1. Reagents and Chemicals

Starch@MNPs were synthesized chemically in Mersin University Environmental Engineering laboratory. Firstly 3 g of starch was dispersed in 300 mL of deionized water at  $100^\circ\text{C}$  for 5 minutes. Then 12.61 g of  $\text{FeSO}_4 \cdot 7\text{H}_2\text{O}$  and 11 g of  $\text{FeCl}_3$  were dissolved in 300 mL of deionized water under a nitrogen atmosphere. When the temperature of the solution reached  $85^\circ\text{C}$ , 35 mL of a 25% purity ammonia ( $\text{NH}_3$ ) solution and 300 mL of starch solution were added and exposed to nitrogen gas for 30 minutes. The obtained black starch- $\text{Fe}_3\text{O}_4$  particles were washed with deionized water until neutral pH and separated from the reaction solution by means of neodymium magnets (Figure 1).



Figure 1. Synthesis steps of Starch- $\text{Fe}_3\text{O}_4$  particles

### 2.3. Adsorbent Characterization

Particle sizes and their morphology of synthesized Starch@MNPs were characterized by a Scanning Electron Microscope (SEM). The characterizations and elemental analysis of the adsorbents were analyzed by FTIR (Fourier Transform Infrared Spectrophotometer) and Energy Dispersive X-Ray Analysis (EDX) techniques.

## 2.4. Adsorption Experiments

Batch adsorption studies were carried out in 50 mL flasks using an orbital shaker at 200 rpm and at room temperature ( $25 \pm 1^\circ\text{C}$ ). The pH of the solutions was adjusted by using 0.1M HCl and 0.1M NaOH solutions.

After the adsorption reaction, the magnetic Starch@MNPs were removed from the solution by precipitation with a magnet, and the solutions were centrifuged by using a centrifuge. Cr(VI) analyses were performed in supernatants to determine the sorption capacities of the adsorbent particles.

The effect of pH on the adsorption of Cr(VI) ions was studied by mixing 1.5 g/L adsorbent concentration with 10 mg/L initial Cr(VI) concentration in 60 min. The pH of the solutions was adjusted at the initial pH of 2.0-10.0 range to determine the effect of pH on the adsorption. Experiments were also carried out at different adsorbent concentrations of 0.3-5.0 g/L at constant pH (optimum) to determine optimum adsorbent concentrations. Similarly, different Cr(VI) concentrations of solutions (2.5-80 mg/L) and reaction times (5-120 min) to find optimal conditions were conducted. The kinetic studies of Cr(VI) adsorption on Starch@MNPs were carried out by adding these adsorbents into the solutions containing Cr(VI) ions in optimum concentration and measuring the Cr(VI) concentration with time.

The adsorption capacities of adsorbents ( $q$ , mg/g) for Cr(VI) ions were calculated according to Equation 1;

$$q = (C_0 + C_e)/M \quad (1)$$

where;  $C_0$  and  $C_e$  are the initial and the equilibrium concentrations of Cr(VI) (mg/L),  $V$  is the solution volume (L), and  $M$  is the mass of the adsorbent (g/L).

## 2.5. Adsorption Kinetics

Adsorption kinetics describe the change of adsorption capacity with time. The most commonly used models developed for the purpose of explaining the adsorption kinetics are pseudo-first-order, pseudo-second-order and intra-particle diffusion. The first-order kinetic model introduced by Lagergren has been applied for the initial stages in which the adsorption process has not yet reached its equilibrium. This equation is as follows [4] (Equation 2).

$$\log(q_e - q_t) = \log(q_e) - (k_1/2.303).t \quad (2)$$

In this equation,  $q_e$  and  $q_t$  (mg/g) show the amounts of adsorbate on the adsorbent at equilibrium and at any time of  $t$ .  $k_1$  is the first-order sorption constant (1/min).

The second order kinetic model which is in harmony with the speed control mechanism throughout the adsorption period, is as follows [5] (Equation 3).

$$t/q_t = 1/(k_2q_e^2) + (t/q_e) \quad (3)$$

In this equation,  $k_2$  is pseudo second-order sorption constant (g/mg.min). In order to design of adsorption applications, this sorption kinetics are so important.

The intra-particle diffusion model has been developed by Weber and Morris [6] (Equation 4);

$$q_e = k_p t_e^{0.5} + C \quad (4)$$

In this equation,  $k_p$  is intra-particle diffusion model rate constant for (mg/g  $^{1/2}$ );  $t_{0.5}$ : half time (min);  $C$ : equilibrium ratio constant for intra-particle diffusion model.

## 2.6. Adsorption Isotherms

The equilibrium data of adsorption processes were analyzed using the Langmuir (Equation 5), Freundlich (Equation 6), and Temkin (Equation 7, 8) adsorption isotherm models

$$1/q_e = 1/bq_m C_e + 1/q_m \quad (5)$$

$$\ln q_e = \ln K_F + 1/n \cdot \ln C_e \quad (6)$$

where,  $q_e$  (mg/g) is adsorption capacity of the adsorbent in equilibrium,  $C_e$  (mg/L) is the concentration of Cr(VI) in equilibrium,  $q_m$  (mg/g) is the maximum adsorption capacities of adsorbents,  $K_F$  and  $K_L$  are the Freundlich and Langmuir coefficients and  $n$  is the Freundlich exponent.

$$q_e = B \ln A_T + B \ln C_e \quad (7)$$

$$B = RT/b_t \quad (8)$$

$b_t$ : Temkin isotherm constant (J/mol);  $A_T$ : Equilibrium binding constant (L/g);  $T$ : Temperature ( $^{\circ}$ K)

### 3. RESULTS AND DISCUSSIONS

#### 3.1. Characterization of Starch-Fe<sub>3</sub>O<sub>4</sub> Nanoparticles

Morphological study of the as-prepared nanoparticles was carried out using SEM. The SEM results were shown in Figure 2 (a-d). In the SEM analysis results, it can be shown showed that Starch@MNPs have a porous structure before the adsorption, and this porous structure decreased after the adsorption process. The pores on the surface of Starch@MNPs closed and the particles tended to stick together and agglomerate after the adsorption. Cr(VI) penetrated both into the particles and on their surface. SEM results also showed that average dimensions of Starch-Fe<sub>3</sub>O<sub>4</sub> nanoparticles was 2. 271  $\mu$ m.

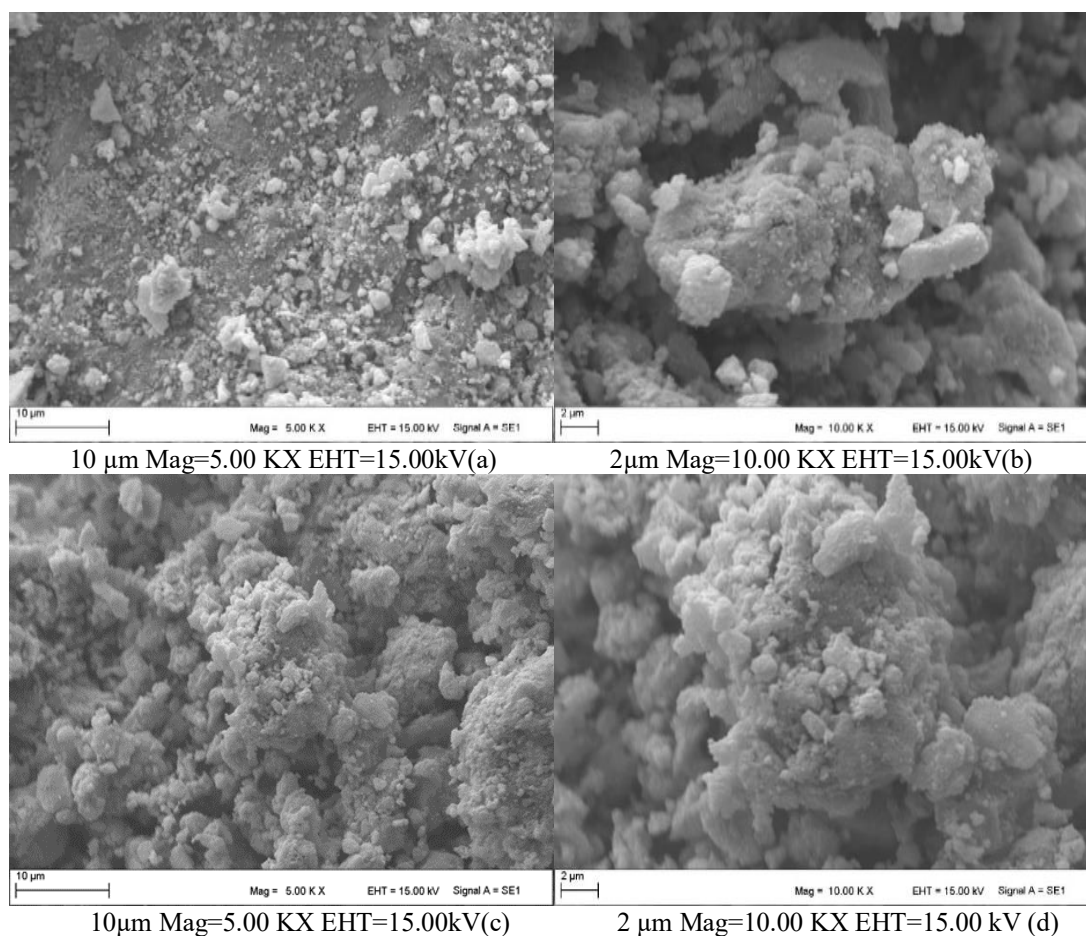


Figure 2. SEM images of Starch-Fe<sub>3</sub>O<sub>4</sub>

In order to determine the material composition, EDX spectrum of Starch@MNPs was obtained and shown in Figure 3. According to EDX results, iron (75.13%) and oxygen (20.87%) constitute the largest part of the total particle mass. The other parts of the particles consisted of carbon (3.55 %) and chromium (0.45 %).

The FTIR spectrum of the raw Fe<sub>3</sub>O<sub>4</sub>, and Starch-Fe<sub>3</sub>O<sub>4</sub> before and after the adsorption were shown in Figure 4. The vibration peaks observed at 539 cm<sup>-1</sup>, 541 cm<sup>-1</sup> and 543 cm<sup>-1</sup> are thought to belong to the characteristic of magnetite and Fe-O bonds in Fe<sub>3</sub>O<sub>4</sub> crystal structure [7, 8]. The vibration peaks appeared at 3174.59 cm<sup>-1</sup>, 3228.11 cm<sup>-1</sup>, 2900.48 cm<sup>-1</sup> and 1629.80 cm<sup>-1</sup> are assigned to the vibrations of hydrogen-bonded water molecules adsorbed on the surface and O-H bending vibration [9, 10]. The peaks at 1077.94 cm<sup>-1</sup>, 1021.46 cm<sup>-1</sup> and 1014.81 cm<sup>-1</sup> are assigned to specifically adsorbed sulphate groups [7].

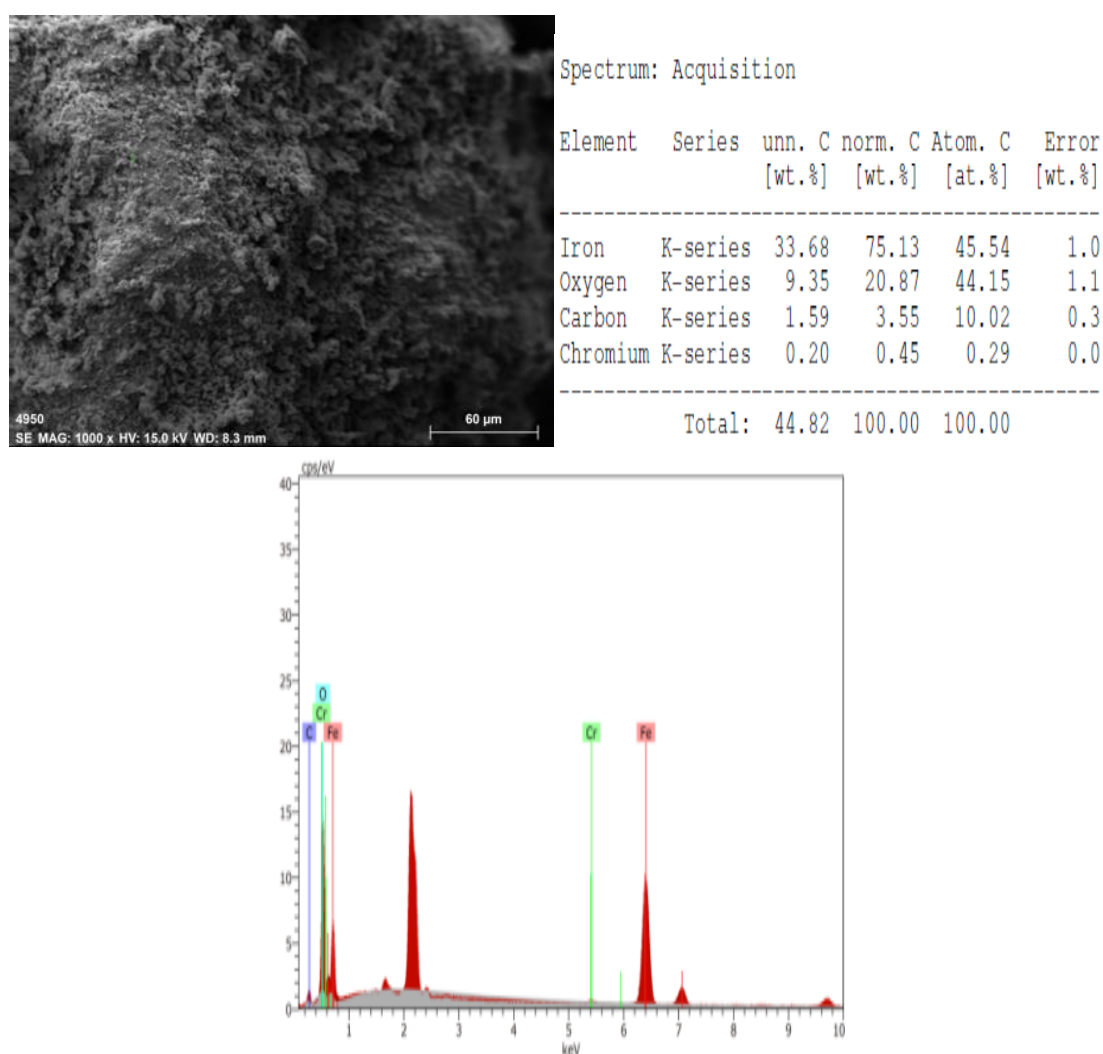


Figure 3. EDX analysis after adsorption

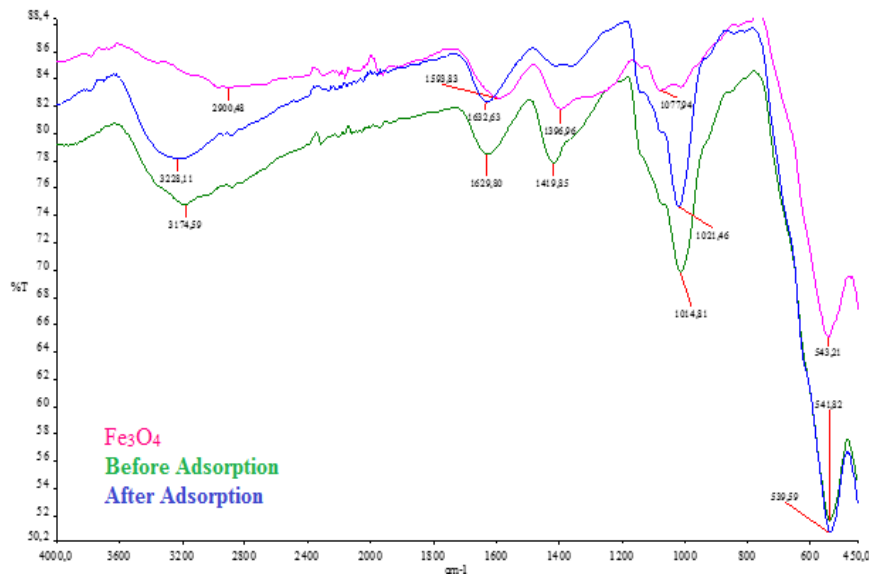


Figure 4. FTIR spectrum of Starch-Fe<sub>3</sub>O<sub>4</sub> particles

### 3.2. Cr(VI) Adsorption Studies

#### 3.2.1. Effect of pH on Cr(VI) removal

The effect of pH on the adsorption of Cr(VI) by using Starch@MNPs composite was determined by using 10 mg/L initial Cr(VI) concentration, 1.5 g/L nanocomposite dose, contact time of 5-60 min. The general trends for the removal results of Cr(VI) ions reflected a continuous decrease in the removal efficiency percentage with increasing the pH values from pH 2 to 10 (Figure 5).

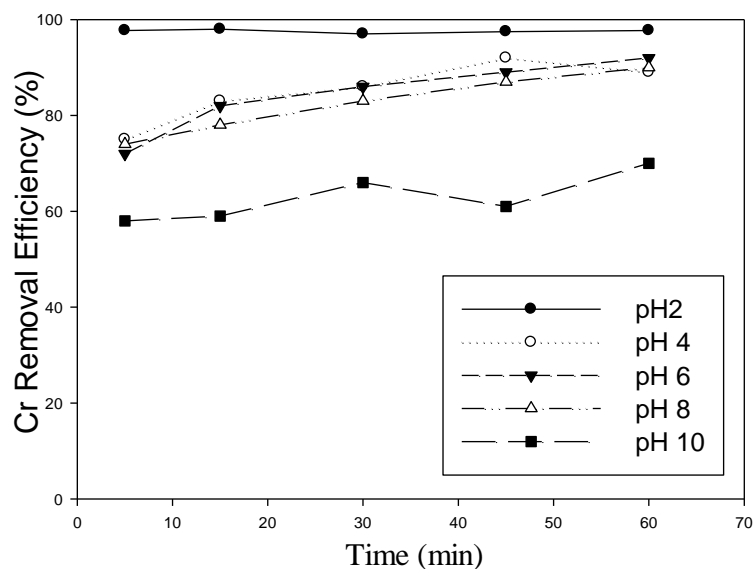


Figure 5. Effect of pH on Cr(VI) removal (Cr(VI) concentration:10 mg/L, nanocomposite dose 1,5 g/L-contact time 5-60 min, T:25°C)

The maximum Cr(VI) removal efficiency was obtained at pH 4.0 as 92 %. It was determined that the Cr(VI) removal efficiency of Starch@MNPs nanocomposite was higher at low pH range of 2.0-8.0, and

decreased with increasing pH. This is due to the higher solubility of heavy metal ions in water at low pH values. As the presence of heavy metal ions in water increased, removal efficiencies were also increased [11].

### 3.2.2. Effect of nanocomposite concentration on Cr(VI) removal

The effect of the adsorbent concentration on the Cr(VI) adsorption by using Starch@MNPs nanocomposites was investigated in the initial Cr(VI) concentration of 10 mg/L, contact time of 60 min and pH 4.0. Adsorbed Cr(VI) concentrations for different nanocomposite concentrations (0.3-5 g/L) were shown in Figure 6 as percentage removal efficiency.

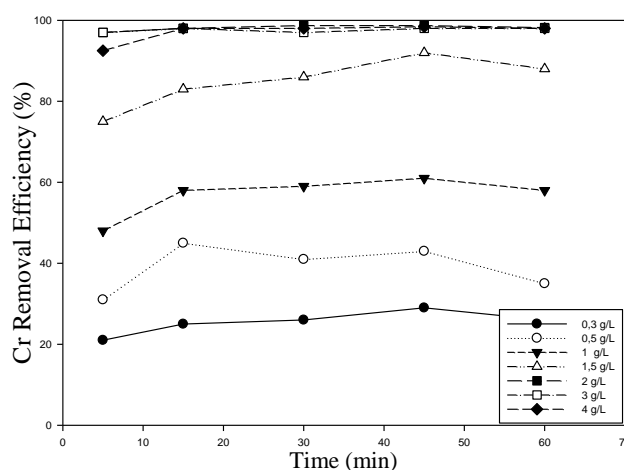


**Figure 6.** Effect of nanocomposite concentration on Cr(VI) removal (Cr (VI):10 mg/L, pH:4.0, contact time: 5-60 min, T:25°C)

As shown in Fig. 6, the maximum Cr (VI) removal was obtained at 2.0 and 3.0 g/L nanocomposite concentrations. Maximum removal efficiency of 97% was achieved in the first 15 minutes at 2.0 g/L Starch-Fe<sub>3</sub>O<sub>4</sub> concentration while, it did not change with time significantly. The lowest Cr (VI) removal efficiency (21-26%) was obtained at the lowest adsorbent concentration of 0.3g/L.

### 3.2.3. Effect of initial Cr(VI) concentration on Cr(VI) removal

The effect of the initial Cr (VI) concentration on Cr (VI) removal was carried out at different Cr (VI) concentrations in the range of 2.5-80 mg/L (adsorbent concentration: 2.0 g/L, pH:4.0 and contact time: 5-120 min). The Cr (VI) removal efficiencies with different initial Cr (VI) concentrations were shown in Figure 7. As shown in Figure 7, it was observed that Cr(VI) removal efficiency decreased with increasing of initial Cr(VI) concentration, and the highest removal efficiency was obtained in 10 mg Cr(VI)/L as 98%.

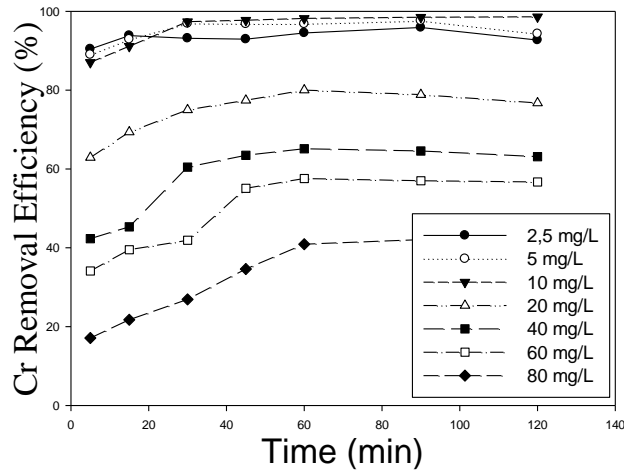


Figure 7. Effect of initial Cr(VI) concentration on Cr(VI) removal (adsorbent concentration: 2 g/L, pH:4.0, contact time: 5-120 min, T:25°C)

### 3.2.4. Effect of contact time on Cr(VI) removal

The effect of contact time on the adsorption of Cr (VI) ions on Starch@MNPs nanocomposite was investigated under optimum conditions of pH 4.0, nanocomposite concentration of 2.0 g/L and Cr(VI) concentration of 2.5-80 mg/L. According to results seen in the Figure 8, maximum Cr(VI) removal efficiency was obtained generally in the first 45 min, and the removal efficiencies did not change significantly with increasing of time.

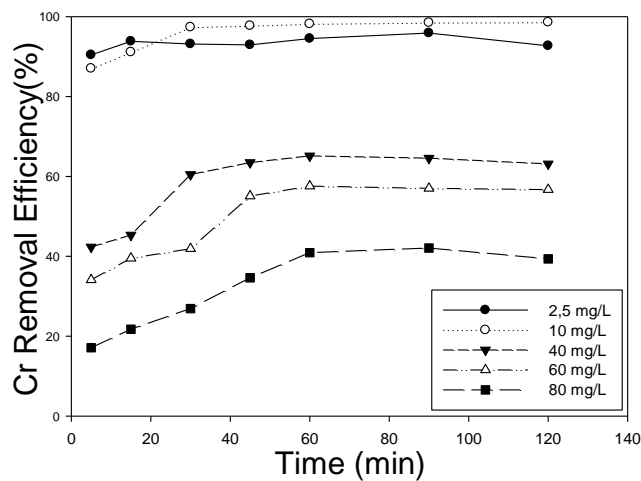
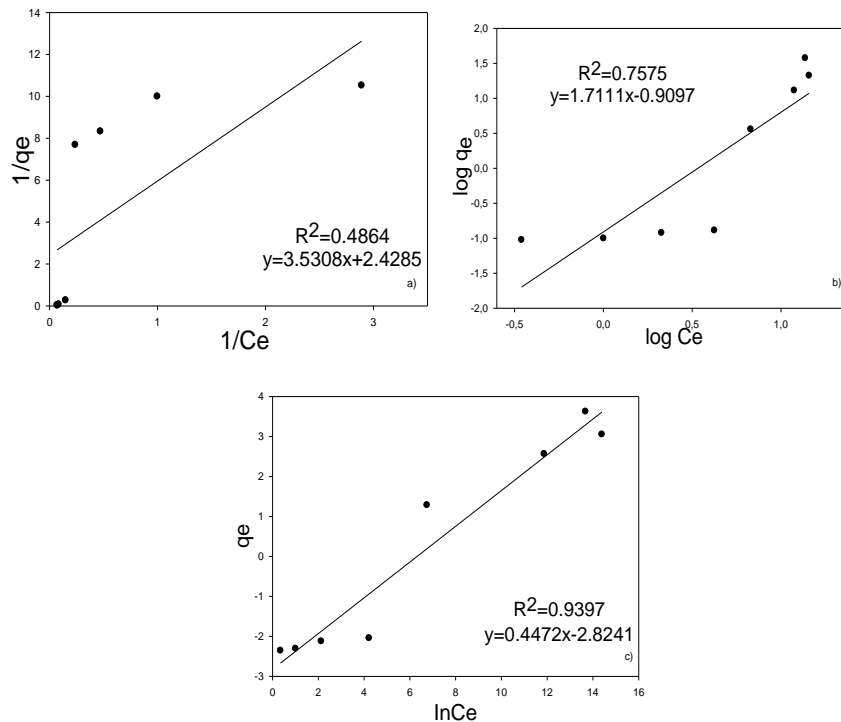


Figure 8. Contact time effect on Cr(VI) removal (adsorbent concentration: 2 g/L, pH:4.0, Cr (VI) concentration: 2.5-80 mg/L, T:25°C)

### 3.3. Adsorption Isotherms

In order to determine the sorption performance of an adsorbent for a special compound which is desired to remove with an adsorption process from polluted water/wastewater, several isotherm calculations are carried out, and constant parameters are calculated for tried each isotherm equations. In this study, experimental data were applied to the Langmuir, Freundlich and Temkin isotherm equations to

determine the most suitable isotherm model by using regression analyses. The constant parameters and correlation coefficients ( $R^2$ ) were summarized in Table 1 and Figure 9 (a, b, c).



**Figure 9.** The isotherm modeling result of Cr(VI) adsorption with Strach-Fe<sub>3</sub>O<sub>4</sub> a) Langmuir isotherm, b) Freundlich isotherm, c) Temkin isotherm.

According to the Table 1, it was also observed that the values of  $n$  and  $R_L$  were all less than 1.0 indicating that adsorption Cr (VI) was favorable. The results showed that the degree of fit for the Temkin model was higher than that for the Freundlich and Langmuir models.

**Table 1.** The parameter of isotherm models

Langmuir Isotherm Model		Freundlich Isotherm Model		Temkin Isotherm Model	
$\frac{1}{q_e} = \frac{1}{bq_m C_e} + \frac{1}{q_m}$		$\ln q_e = \ln K_f + \frac{1}{n} \ln C_e$		$q_e = \frac{R \cdot T}{b_T} \cdot \ln(A_T \cdot C_e)$	
$q_m$ (mg/g)	0.280	$K_f$ (mg/g) (L/mg <sup>1/n</sup> )	8.120	$B_T$	0.44
$b$ (L/mg)	1.472	$n$	0.584	$A_T$ (L/g)	1.46
$R_L$	0.271	$R^2$	0.758	$R^2$	0.929
$R^2$	0.486				

$q_e$ : amount of adsorbed material,  $b$ : Langmuir constant,  $C_e$ : equilibrium concentration,  $q_m$ : monolayer adsorption capacity,  $K_f$  and  $n$ : Freundlich constants,  $R$ : constant,  $T$ : temperature,  $b_T$  and  $A_T$ : Temkin isotherm constants.

### 3.4. Adsorption Kinetics

In order to study the mechanism of the adsorption process, kinetic experiments were carried out at 25°C with adsorbent concentration of 2.0 g/L and initial Cr(VI) concentration of 10 mg/L. The adsorption capacities were determined for 5-120 min. The pseudo-first-order, the pseudo second order and

intraparticle diffusion models were used to evaluate the fits of the obtained data. The constant parameters and correlation coefficients (R) were summarized in Table 2 and Figure 10 (a, b and c).

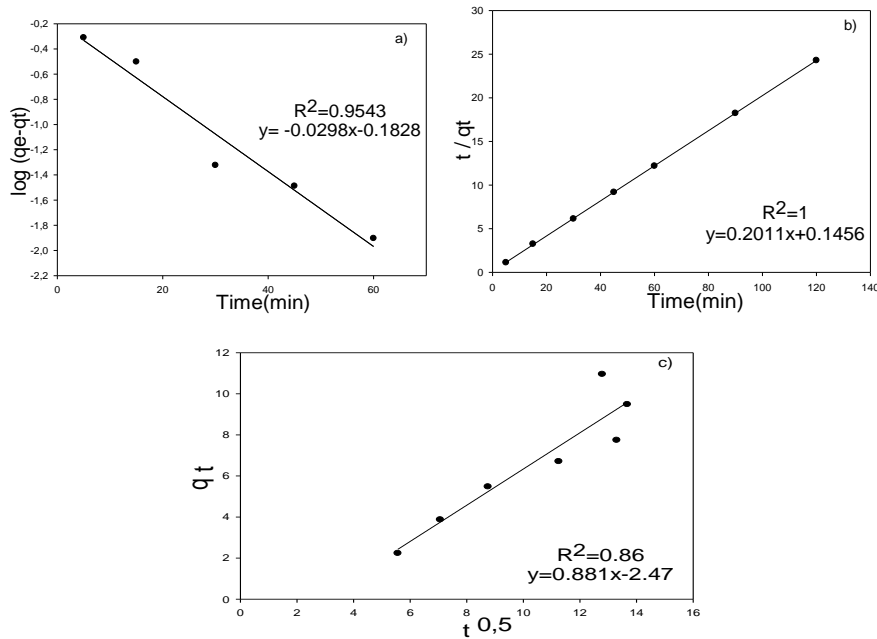


**Figure 10.** a) Pseudo-first-order kinetic model, b) Pseudo-second-order kinetic model, c) Intraparticle diffusion kinetic model.

As can be seen Table 2, correlation coefficient of pseudo-second-order model for Cr(VI) adsorption with Starch-Fe<sub>3</sub>O<sub>4</sub> is larger than correlation coefficients of pseudo-first order and intraparticle diffusion models. Pseudo-second-order model for Cr(VI) adsorption demonstrates the chemisorption may be the rate-limiting step.

**Table 2.** The parameter of kinetic models

Pseudo-First Order Kinetic Model			Pseudo-Second Order Kinetic Model			Intraparticle Diffusion Model		
k <sub>1</sub> (l/min)	q <sub>e</sub> (mg/g)	R <sup>2</sup>	k <sub>2</sub> (l/min)	q <sub>e</sub> (mg/g)	R <sup>2</sup>	k <sub>p</sub> (g.dk <sup>0.5</sup> )	C (mg/g)	R <sup>2</sup>
0.099	0.20	0.954	4.11	0.20	1.00	0.982	3.82	0.86
$\log(q_e - q_t) = \log q_e - \frac{k_1}{2.303} * t$			$\frac{1}{q_t} = \left[ \frac{1}{k_2 * q_e^2} \right] + \frac{1}{q_e} * t$			$q_e = k_p t^{0.5} + C$		

k<sub>1</sub>: the pseudo first-order rate constant, k<sub>2</sub>: the pseudo second-order rate constant, k<sub>p</sub>: intra-particle diffusion rate constant, C: boundary layer thickness.

Data on the removal of Cr(VI) ions by adsorption process obtained from several studies in the literature were given in Table 3. When the results obtained in this study are compared with the results of similar studies in the literature, it is revealed that the results of the isotherm model of this study are compatible with the Temkin isotherm model unlike other studies.

**Table 3.** Studies in the literature about Cr(VI) removal by adsorption

Adsorbent	Adsorption isotherm/kinetic	Efficiency/ Adsorption capacity	Reference
Starch-functionalized magnetite nanoparticles (SMNPs)	Freundlich isotherm Pseudo-second-order kinetic model	pH 2.0 26.6 mg/g	[12]
Starch (MNP <sub>ST</sub> ) magnetite nanoparticles	Langmuir isotherm Pseudo-second-order kinetic model	99.0 mg/g	[13]
Casein (MNP <sub>CS</sub> ) magnetite nanoparticles	Langmuir isotherm Pseudo-second-order kinetic model	87.81 mg/g	[13]
CTAB modified Magnetic nanoparticles (Fe <sub>3</sub> O <sub>4</sub> )	Langmuir isotherm Pseudo-second-order kinetic	6.74 mg/g 95.77%	[14]
Mixed magnetite and maghemite nanoparticles	-	2.4 mg/g 96-99%	[15]
L-Cysteine Functionalized Magnetite (Fe <sub>3</sub> O <sub>4</sub> ) Nanoparticles	Langmuir isotherm Pseudo-second-order kinetic	34.5 mg/g	[16]
RGO/NiO	Langmuir isotherm Pseudo-second-order kinetic model	198 mg/g	[17]
Fe-Cu binary oxide nanoparticles	Freundlich isotherm Pseudo-second-order kinetic	pH 3.0 71.43 mg/g	[18]
Ni <sub>2</sub> O <sub>3</sub> nanoparticles	Pseudo-second-order kinetic	pH 6.0 20.41 mg/g	[19]
Spent tea-supported magnetite (ST/Mag) nanoparticles	Langmuir and Liu isotherm models Pseudo-second-order kinetic	pH 2.0 30 mg/g	[20]
Starch-coated magnetic nanoparticles (Starch@MNPs)	Temkin isotherm model Pseudo-second-order kinetic	pH 4.0 3.8 mg/g 98.2%	This study

#### 4. CONCLUSIONS

In this research, Starch/Fe<sub>3</sub>O<sub>4</sub> nanoparticles were synthesized as adsorbent materials and their removal efficiency on Cr (VI) ions from water was investigated. It was observed that the removal of Cr (VI) at high pH values decreased in comparison with low pH values, and the optimum removal was obtained at pH 4.0. Similarly, optimum process conditions such as adsorbent concentration, initial Cr (VI) concentration and contact time were determined as 2.0 g/L, 10 mg/L and 60 min, respectively. Kinetic studies were carried out to examine the adsorption mechanism, and the correlation coefficients of the first and second degree and intraparticle diffusion kinetics reactions were calculated as 0.954, 1.00 and 0.86, respectively. According to these calculations, Cr (VI) adsorption was more appropriate to the second order kinetic model. In order to determine adsorption isotherm model, Langmuir, Freundlich and Tempkin isotherm equations and their coefficients were interpreted, and best isotherm model was found to be Tempkin equation.

#### REFERENCES

- [1] El-Dib FI, Mohamed DE, El-Shamy OAA, Mishrif MR. Study the adsorption properties of magnetite nanoparticles in the presence of different synthesized surfactants for heavy metal ions removal. Egypt J Pet 2019; 1-7 .

- [2] Ghaseminezhad SM, Shojaosadati SA. Evaluation of the antibacterial activity of Ag/Fe<sub>3</sub>O<sub>4</sub> nanocomposites synthesized using starch. *Carbohydr Polym* 2016; 144: 454–463.
- [3] Hamidian H, Tavakoli T. Preparation of a new Fe<sub>3</sub>O<sub>4</sub>/starch-g-polyester nanocomposite hydrogel and a study on swelling and drug delivery properties. *Carbohydr Polymers* 2016; 144: 140–148.
- [4] Lagergren S. About the theory of so-called adsorption of soluble substance. *Kung Sven Vetén Hand* 1898; 24: 1-39.
- [5] Ho YS, McKay G. Pseudo-second order model for sorption processes. *Process Biochem* 1999; 34: 451-465.
- [6] Weber Jr WJ, Morriss JC. Kinetics of adsorption on carbon from solution. *J Sanit Eng Div* 1963; 89: 31–60.
- [7] Cornwell RM, Schwertmann U. *The Iron Oxides: Structure, Properties, Reactions, Occurrences and Uses*. 2nd. Ed. Wiley-VCH, 2006.
- [8] Zheng L, Su W, Qi Z, Xu Y, Zhou M, Xie Y. First-order metal–insulator transition and infrared identification of shape-controlled magnetite nanocrystals. *Nanotechnology* 2011; 22: 485-706.
- [9] Gotić M, Musić S. FT-IR and FE-SEM investigation of iron oxides precipitated from FeSO<sub>4</sub> solutions. *J Mol Struct* 2007; 834: 445-453.
- [10] Holland H, Yamaura M. Synthesis of magnetite nanoparticles by microwave irradiation and characterization. In: *Internacional Latin American Conference On Powder Technology*; 08-10 November 2009; Atibaia SP, Brazil. Pp. 1-6.
- [11] Uysal Y, Dergi ZÇ, Şimşek R. Atıksudan Mn<sup>+2</sup> iyonlarının pektin kaplı nano manyetit kullanılarak giderilmesi. In: *International Symposium on Urban Water and Wastewater Management*; 25-27 October 2018; Denizli, Turkey. pp. 915-916.
- [12] Singh PN, Tiwary D, Sinha I. Starch-functionalized magnetite nanoparticles for hexavalent chromium removal from aqueous solutions. *Desalin Water Treat* 2016; 57: 12608-12619.
- [13] Somu P, Kannan U, Paul S. Biomolecule functionalized magnetite nanoparticles efficiently adsorb and remove heavy metals from contaminated water. *J Chem Technol Biotechnol* 2019; 94: 2009-2022.
- [14] Elfeky SA, Mahmoud SE, Youssef AF. Applications of CTAB modified magnetic nanoparticles for removal of chromium (VI) from contaminated water. *J Adv Res* 2017; 8:435-443.
- [15] Chowdhury SR, Yanful EK. Arsenic and chromium removal by mixed magnetite–maghemite nanoparticles and the effect of phosphate on removal. *J Environ Manage* 2010; 91:2238-2247.
- [16] Bagbi Y, Sarswat A, Mohan D, Pandey A, Solanki PR. Lead and chromium adsorption from water using L-Cysteine functionalized magnetite (Fe<sub>3</sub>O<sub>4</sub>) nanoparticles. *Sci Rep* 2017; 7:7672.
- [17] Zhang K, Li H, Xu X, Yu H. Synthesis of reduced graphene oxide/NiO nanocomposites for the removal of Cr(VI) from aqueous water by adsorption. *Micropor Mesopor Mat* 2018; 255: 7–14.

- [18] Khan SU, Zaidi R, Hassan SZ, Farooqi IH, Azam A. Application of Fe-Cu binary oxide nanoparticles for the removal of hexavalent chromium from aqueous solution. *Water Sci and Technol* 2016; 165-175.
- [19] Dey S, Bhattacharjee S, Chaudhuri MG, Bose RS, Halder S, Ghosh, CK. Synthesis of pure nickel (III) oxide nanoparticles at room temperature for Cr(VI) ion removal. *RSC Advances* 2015; 5:54717–54726.
- [20] Babaei AA, Ahmadi M, Goudarzi G, Jaafarzadeh N, Baboli Z. Adsorption of chromium (VI) from saline wastewater using spent tea-supported magnetite nanoparticle. *Desalin Water Treat* 2015; 57:12244–12256.